

IJTC2009-15130

ANALYSIS OF THE BÉNARD CELL-LIKE WORN SURFACE TYPE OCCURRED DURING OIL-LUBRICATED SLIDING CONTACT

Jen Fin Lin/National Cheng Kung University

Hsiao Yeh Chu/Kun Shan University
hsiaoyeh@mail.ksu.edu.tw

ABSTRACT

Scuffing wear is usually used as an important indication of the initiation of lubrication failure. Components with scuffing wear should be readily replaced in order to avoid severe wear. This paper observed the change of surface structure in the scuffed area of the worn surface of oil-lubricated vanes-on-ring specimens from a microscopic and nano-scale observation and material characterization. There existed a kind of Bénard cell-like special surface shape found from the observation of the TEM image of the scuffed surface. In order to see whether there was very hot surface temperature to produce Benard cell, structure of the surface ferrous material was used as an indirect evidence of high temperature. It showed that the temperature in the scuffed area suffered a very high temperature which was over 800°C from the TEM Result. It showed that very strong fluid convection or even evaporation may occur inside the scuffed surface. The material strength of the scuffed surface would be much lower due to this high temperature. The oil pressure of that high temperature area was also very high. These factors made it possible to form the Bénard cell structure in microscale.

INTRODUCTION

Scuffing wear is considered as a local phenomenon between two mutually sliding surfaces due to the surface temperature reaches the welding temperature of the two surfaces at the asperity contact area. Generally, friction force, noise, and chattering will also increase as scuffing wear occurs. The mechanism of scuffing wear is not clearly known yet. Markov and Kelley [1] described the meaning of seizure, scoring, scuffing, and galling historically. In order to avoid the initiation of scuffing during element contact in a machine, some research showed that the addition of nano-particles into lubricating oil would be effective in anti-seizure and increase the load to initiate scuffing wear [2-4]. These nano-particle contained oils can reduce wear of surfaces since it can prohibit metal to metal contact effectively. Grew and Cameron [5] described the chemical reaction of surfacial materials. They explained the relations between additives and scuffing wear. Some research paper concerning scuffing models and related factors are discussed [6-8]. Two methods on the prediction

criteria of scuffing wear initiation were proposed: critical temperature model [9] and critical Friction power intensity model [10].

Evans et al. [11-12] conducted mineral oil lubricated tapered roller bearings tests with and without sulfur- and phosphorus-containing gear oil additives. They observed the boundary-lubricated bearing surfaces by transmission electron microscopy. Focused ion beam (FIB) milling technique was used. They found that the characteristics of oxide surface layers and micro-cracks on the tested bearing surfaces were evaluated and found to depend on lubrication conditions. Two types of oxide surface layers (or boundary films) were characterized in cross section. They discussed in detail on the relation between oxide layer and substrate by the crystal structure and element category and percentage. Hershberger et al. [13] discussed the formation of austenite during scuffing failure of SAE 4340 steel through the SEM cross-section images. They proved that there was obvious plastic deformation in the scuffed areas after scuffing initiated. Edrissy et al. [14] also found that there was severe plastic deformation on the scuffed surface from the cross-sectional SEM images. The delamination of the tribolayers was the principal source of material removal during scuffing from their study. In these former studies, the cause or evidence that gives rise to the occurrence of scuffing was not explained clearly. In our research, we conducted a wear experiment and observe the surface microstructure. The morphology and content of the surface were analyzed and discussion on the relationship between these observations and scuffing phenomenon were thrown in this paper.

EXPERIMENTAL DETAIL

The type of the wear test conducted in our study was vanes-on-ring with uni-directional rotation on Falex-6 wear tester. Fig.1 shows the 3D illustrations of the vanes-on-ring test specimens and adapter. The reason for selecting vanes-on-ring test configuration was that it is similar to the configuration of the engine piston ring and cylinder. The material of the upper specimen (vanes) was SKD11 tool steel with hardness and surface roughness of HRC29.8~HRC36.6 and $0.499 \pm 0.131 \mu\text{m}$, respectively. The lower specimen (ring) was SKD61 tool steel with hardness and surface roughness are HRC52.3~HRC56.8

and $0.044 \pm 0.016 \mu\text{m}$, respectively. Chemical compositions of these two materials are listed in Table 1. The contact pressure and the sliding velocity are 5.11 MPa and 4.867 m/s, respectively. The test time period is 5400 seconds. The lubricating oil used was CPC Circulation Oil R68. The base oil of R68 is Paraffinic Distillate.

Table 1 Chemical composition of the upper and lower specimens

| Material (Specimen) | Chemical compositions (wt%) | | | | | | | |
|---------------------|-----------------------------|---------|------|-------|-------|-----------|---------|---------|
| | C | Si | Mn | P | S | Cr | Mo | V |
| SKD11 (Upper) | 1.4~1.6 | <0.4 | <0.5 | <0.03 | <0.03 | 11.0~13.0 | 0.8~1.2 | 0.2~0.5 |
| SKD61 (Lower) | 0.32~0.42 | 0.8~1.2 | <0.5 | <0.03 | <0.03 | 4.5~5.5 | 1.0~1.5 | 0.8~1.2 |

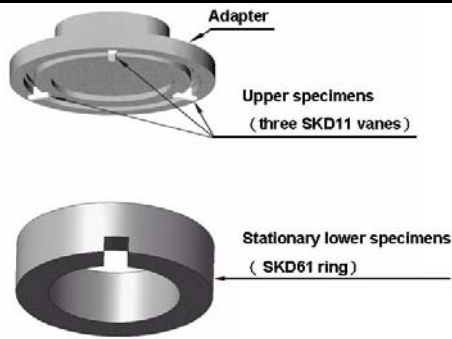


Fig.1 3D illustrations of the vanes-on-ring test specimens and adapter

FIB, EDS, and TEM were used in order to provide the surface and cross-section images of the scuffed area, as well as compositions and crystalline structures information for further study use.

Results and Discussion

The worn surface of the lower specimen was observed by FIB. Fig.2 showed that honeycombed surface was observed. The shape was similar to the Bénard cell. Bénard cell is a pattern of convection in the form of hexagonal cells which was first observed by Henri Bénard [15]. The shape of these hexagonal cells looks like the image shown in Fig.3 [16]. Bénard determined correctly that warm fluid was flowing up in the centres of the convection cells, and down at the hexagonal boundaries in Fig.3 [16]. SEM, EDS, XRD, FIB, and TEM were used in our study to analyze and explain this special wear type. We proposed a possible mechanism for the explanation on the formation of such peculiar condition: The surface was heated by sliding wear. The temperature of the worn region can be at the range of 738°C to 1494°C from the evidence of TEM result of selected area diffraction. It showed that both $\gamma\text{-Fe}$ and $\alpha\text{-Fe}$ were all found near the scuffed surface; as shown in Fig.4(a). But only $\alpha\text{-Fe}$ was found inside the substrate of the unscuffed surface; as shown in Fig.4(b). $\gamma\text{-Fe}$ can only be formed at the temperature range of 738°C to 1494°C from the phase diagram of Fe-Fe₃C. When the asperity peaks of the

upper and lower specimens collided one another, the material near these collision areas of the worn surface became softened or melted due to very high flash temperature caused by friction dissipated energy released during collision. However, the temperature on top of the surface was quickly cooled down because the lubricating oil between the two mutually sliding specimens would absorb some heat from the surface after the contact collision of the asperity peaks. The oil would become boiling or cavitating locally. Therefore, the temperature on the outer surface is lower than the melted or softened inner subsurface. Bénard convection was thus possible to form. Meanwhile, since the oil was trapped inside the two mutually sliding asperities of the surfaces, the boiling or cavitating oil would change from liquid phase to gas phase, which would produce oil gas bubbles in the contact area. The occurrence of those bubbles caused by phase change from liquid to gas between the two specimens' surfaces was like explosions at those local area surfaces, which caused a lot of oil gas bubble imprints on the specimen's surfaces and enabled Bénard cell-like worn surface type more obvious to be observed. Moreover, it was observed that there are microcracks on the bottom of the Bénard cell-like microstructure from the FIB images of Fig.2. This would become debris if the crack propagated and finally was peeled off. This is a reason why scuffing wear was often accompanied with severe wear loss.

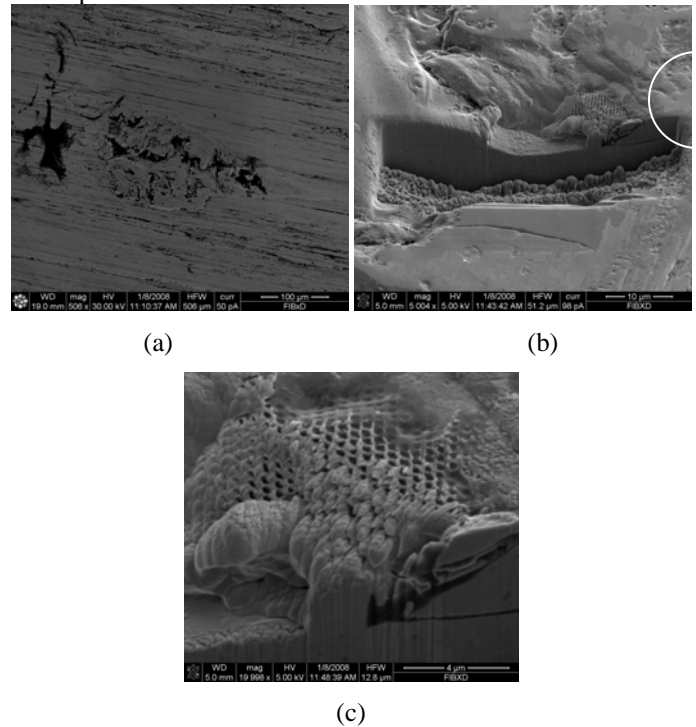


Fig.2 FIB images of the Bénard cell-like worn surface type. (a) The scuffed cavity located at the worn spot; (b) FIB milling technique applied inside the worn spot; (c) Magnification of the Bénard cell-like worn surface shown in (b).

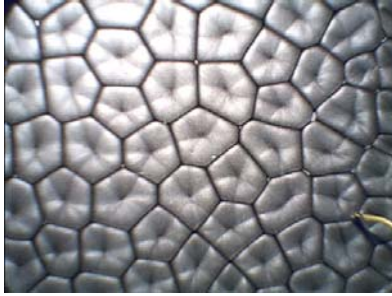
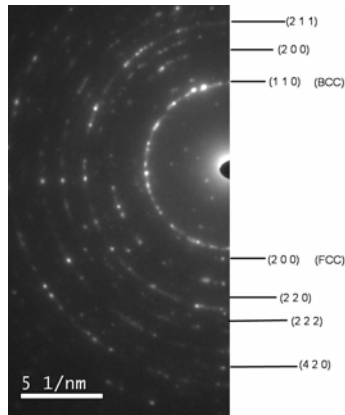
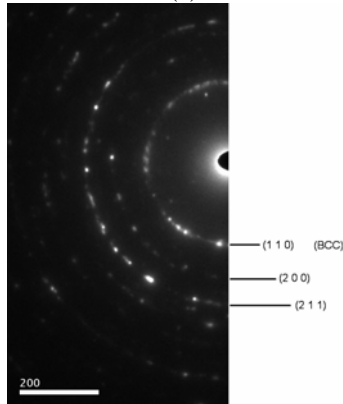


Fig.3 Honeycomb-like cell pattern observed in Bénard convection.



(a)



(b)

Fig.4 TEM selected area diffraction of the worn specimens. The locations are (a) near the scuffed surface. (b) inside the subsurface of the scuffed area.

CONCLUSIONS

In our paper, the Bénard cell-like microstructure on the scuffed surface is found after oil lubricated wear tests. This special texture is assumed to be formed by the very high temperature of the real asperity contact areas from the evidence of the TEM analysis of the scuffed worn surface. The surface of the asperity contact areas is softened or even melted. The Bénard cell-like microstructure is the result of both natural convection and the imprints of the oil gas bubbles. It is also observed that there are microcracks on the bottom of the

Bénard cell-like microstructure, which is a reason why scuffing wear was often accompanied with severe wear loss.

REFERENCES

- [1] Markov, D., Kelly, D., 2000, "Mechanisms of adhesion-initiated catastrophic wear: Pure sliding," *Wear*, **239**, pp.189-210.
- [2] Li, B., Wang, X., Liu, W., Xue, Q., 2006, "Tribiochemistry and antiwear mechanism of organic-inorganic nanoparticles as lubricant additives," *Tribology Letters*, **22**(1), pp. 79-84.
- [3] Qiu, S., Zhou, Z., Dong, J., Chen, G., 2001, "Preparation of Ni nanoparticles and evaluation of their tribological performance as potential additives in oils," *Journal of Tribology*, **123**(3), pp. 441-443.
- [4] Piekoszewski, W., Szczerek, M., Tuszynski, W., 2001, "The action of lubricants under extreme pressure conditions in a modified," *Wear*, **249**, pp. 188-193.
- [5] Grew, W.J.S., Cameron, A., 1972, "Thermodynamics of boundary lubrication and scuffing," *Proc. Roy. Soc. Lond. A.*, **327**, pp. 47-59.
- [6] Bowman, W.F., Stachowiak, G.W., 1996, "A review of scuffing models," *Tribology Letters*, **2**, pp. 113-131.
- [7] Ludema, K.C., 1984, "A review of scuffing and running-in of lubricated surfaces with asperities and oxides in perspective," *Wear*, **100**, pp. 315-331.
- [8] Dyson, A., 1975, "Scuffing - a review, Part 1 and Part 2," *Tribology International*, **8**, pp. 77-87, 117-122.
- [9] Blok, H., 1937, "Theoretical Study of Temperature Rise at Surfaces of Actual Contact under Oiliness Lubricating Conditions," *Inst. Mech. Engrs.*, **2**, pp. 222-235.
- [10] Matveevsky, R.M., 1992, "Friction power as a criterion of seizure with sliding lubricated contact," *Wear*, **155**, pp. 1-5.
- [11] Evans, R.D., More, K.L., Darragh, C.V., H.P. Nixon, 2005, "Transmission electron microscopy of boundary-lubricated bearing surfaces. Part II: Mineral oil lubricant with sulfur- and phosphorus-containing gear oil additives," *Tribology Transactions*, **48**, pp. 299-307.
- [12] Evans, R.D., More, K.L., Darragh, C.V., Nixon, H.P., 2004, "Transmission electron microscopy of boundary-lubricated bearing surfaces. Part I: Mineral oil lubricant," *Tribology Transactions*, **47**, pp. 430-439.
- [13] Hershberger, J., Ajayi, O.O., Zhang, J., Yoon, H., Fenske, G.R., 2004, "Formation of austenite during scuffing failure of SAE 4340 steel," *Wear*, **256**, pp. 159-167.
- [14] Edrissy, A., Perry, T., Alpas, A.T., 2005, "Investigation of scuffing damage in aluminum engines with thermal spray coatings," *Wear*, **259**, pp. 1056-1062.
- [15] Bénard, H., 1900, "Les tourbillons cellulaires dans une nappe liquide," *Rev. G'en. Sci. Pure Appl.*, **11**, pp. 1261-71.
- [16] Maroto, J.A., Pérez-Muñuzuri, V., Romero-Cano, M.S., 2007, "Introductory analysis of Bénard-Marangoni convection," *Eur. J. Phys.*, **28**, pp. 311-320.